WING ANGLE OF ATTACK FOR ZERO LIFT AT SUBCRITICAL MACH NUMBERS

1. NOTATION AND UNITS

		SI	*British*
A	aspect ratio, $b/\bar{c}$		
a_1	lift-curve slope	degree^{-1}	degree^{-1}
b	wing span	m	ft
C_L	total lift coefficient		
C_{LLT0}	local lift coefficient due to effective twist at zero C_L		
C_{LTA}	lift coefficient due to unit effective twist of type A, see Item No. 83040 (Derivation 39) and Sketch 3.2	degree^{-1}	degree^{-1}
C_{LTB}	lift coefficient due to unit effective twist of type B, see Item No. 83040 (Derivation 39) and Sketch 3.3	degree^{-1}	degree^{-1}
c	local chord	m	ft
$\bar{c}$	geometric mean chord, $\int_0^1 c\,d\eta$	m	ft
c_r	wing root (centre-line) chord	m	ft
c_t	wing tip chord	m	ft
N	number of linear twist segments		
x	streamwise co-ordinate, positive aft	m	ft
z_c	camber ordinate	m	ft
α_r	angle of attack of wing root section	degree	degree
α_{0r}	angle of attack of wing root section for zero C_L	degree	degree
$(\alpha_{0r})_1$	contribution to α_{0r} due to camber for untwisted wing with camber line corresponding to that for root section	degree	degree
$(\alpha_{0r})_2$	contribution to α_{0r} due to effective twist	degree	degree
$(\alpha_{0r})_\infty$	local two-dimensional angle of attack for zero lift	degree	degree

Issued November 1987
Reprinted with Amendment A, January 1999
This page Amendment A

δ	local geometric twist (angle of local chord relative to root chord, positive leading-edge up)	degree	degree
δ_c	local camber-dependent twist relative to wing root, Equation (3.4)	degree	degree
δ_e	effective wing twist, Equation (3.5)	degree	degree
δ_{et}	value of δ_e at tip	degree	degree
δ'_{et}	equivalent linear tip twist, Equation (3.11)	degree	degree
η	spanwise distance from root as fraction of semi-span		
η_K, η_{Ki}	value of η at intersection of linear twist segments		
θ	effective local twist relative to datum value at η_K in linear segment representation (positive leading-edge up)	degree	degree
θ_A	effective root twist relative to datum value at η_K in linear segment representation, see Sketch 3.2 (positive root leading-edge up)	degree	degree
θ_B	effective tip twist relative to datum value at η_K in linear segment representation, see Sketch 3.3 (positive tip leading-edge up)	degree	degree
$\Lambda_{¼}$	sweepback of ¼-chord line	degree	degree
λ	taper ratio, c_t/c_r		

Subscripts

expt	denotes experimental value
i	denotes *i*'th linear twist segment of type B used in calculating effective twist (i = 1 to n)
n	denotes *n*'th linear twist segment of type B (n = 1 to N – 1)
pred	denotes predicted value
r	denotes value at wing root
t	denotes value at wing tip
th	denotes approximate theoretical value
∞	denotes wing sectional value in two-dimensional flow
η	denotes value at spanwise location η

2. INTRODUCTION

This Item provides a simple semi-empirical method for estimating wing angle of attack for zero lift at subcritical Mach numbers.

The method, presented in Section 3, consists of separate estimations of two contributions to zero-lift angle of attack. The first is due to camber, taken for reference purposes as that corresponding to the wing root section and assumed unchanged across the span. The second is due to the combined effects of geometric twist and "camber-dependent" twist associated with spanwise changes in camber. The method, although based on low-speed considerations, is applicable to any subcritical Mach number.

The contribution, $(\alpha_{0r})_1$, due to the reference camber line at the wing root (Section 3.2) is based on an approximate theoretical estimate for two-dimensional flow, corrected with an empirical factor which is independent of wing planform. Two methods are provided for estimating the remaining contribution, $(\alpha_{0r})_2$, due to "effective wing twist", which combines the effects of geometric and camber-dependent twist (Section 3.3). For linear or monotonic distributions of effective wing twist, the method is based on solutions obtained from extended lifting-line theory, monotonic distributions being treated in terms of equivalent linear distributions. For more complex twist distributions a method involving their representation by a system of linear segments is used.

The applicability and accuracy of the method are discussed in Section 4 and illustrations of typical uses of the Item are given in worked examples in Section 6.

The associated pitching moment at zero lift can be estimated by using Item No. 87001 (Reference 42).

3. WING ANGLE OF ATTACK FOR ZERO LIFT

3.1 General

For the most general case of a cambered and twisted wing the total lift coefficient for an angle of attack referred to the chord of the root (centre-line) section is given by

$$C_L = a_1[\alpha_r - (\alpha_{0r})_1 - (\alpha_{0r})_2], \tag{3.1}$$

so that for zero total lift

$$\alpha_r = \alpha_{0r} = (\alpha_{0r})_1 + (\alpha_{0r})_2. \tag{3.2}$$

In Equation (3.2), α_{0r} is the angle of attack for zero total wing lift, $(\alpha_{0r})_1$ is the contribution to α_{0r} due to the reference camber line and $(\alpha_{0r})_2$ is the contribution due to effective wing twist.

The angle of attack of the root section at zero total wing lift due to twist on an otherwise uncambered wing is $(\alpha_{0r})_2$ and is therefore associated with the condition

$$\int_0^1 (C_{LLT0}c/\bar{c})_\eta \, d\eta = 0 \tag{3.3}$$

where $(C_{LLT0}c/\bar{c})_\eta$ is the local loading at zero total wing lift due to the combined effects of local geometric twist, δ, and local camber-dependent twist, δ_c, which arises for those cases in which the camber line, and

hence the local zero-lift angle of attack, varies across the wing. The local geometric twist is defined as the angle of the local chord relative to the root chord, *i.e.* $\delta = \alpha_\eta - \alpha_r$. The local camber-dependent twist is defined as the difference between the local and root section values of $-(\alpha_0)_\infty$, *i.e.*

$$\delta_c = (\alpha_{0r})_\infty - (\alpha_{0\eta})_\infty . \tag{3.4}$$

The combined, or effective, local twist, δ_e, can be written as

$$\delta_e = \delta + \delta_c = (\alpha_{0r})_\infty - (\alpha_{0\eta})_\infty \tag{3.5}$$

which can be interpreted as the angle of the local zero-lift line relative to that of the root section. The determination of $(\alpha_{0\eta})_\infty$ and $(\alpha_{0r})_\infty$ is carried out by using Equation (3.8) in Section 3.2.

At the wing tip, Equation (3.5) becomes

$$\delta_{et} = \delta_t + (\alpha_{0r})_\infty - (\alpha_{0t})_\infty . \tag{3.6}$$

When the camber line is unchanged across the span, $(\alpha_{0r})_\infty = (\alpha_{0t})_\infty$, and Equation (3.6) reduces to

$$\delta_{et} = \delta_t . \tag{3.7}$$

Procedures for obtaining $(\alpha_{0r})_1$ and $(\alpha_{0r})_2$ from low-speed considerations are presented in Sections 3.2 and 3.3 respectively. The resulting values are, however, applicable over the subcritical Mach number range.

3.2 Evaluation of $(\alpha_{0r})_1$

For aerofoils the angle of attack for zero lift at low speeds is given by

$$(\alpha_0)_\infty = 0.87(\alpha_0)_{\infty th} \tag{3.8}$$

in which $(\alpha_0)_{\infty th}$ is the value obtained by using Item No. 72024 (Derivation 2) and 0.87 is an empirical correction factor obtained from comparisons of $(\alpha_0)_{\infty th}$ with wind-tunnel test data for a large number of aerofoils at low speeds in Derivations 1 and 3 to 11. An improvement in the estimation of $(\alpha_0)_\infty$ is possible by use of the method of Item No. 98011 (Reference 43), where the constant 0.87 is replaced by a viscous correction factor dependent on section geometry, Reynolds number and Mach number. However, it should be noted that the difference in prediction is small in magnitude and of little consequence in the estimation of α_{0r} for a wing.

Analysis of low-speed wind-tunnel test data for untwisted wings with section camber lines unchanged across the span (Derivations 12 to 23, 25 and 26) has shown that planform effects on zero-lift angle are insignificant and that Equation (3.8) still applies. Thus, for the purpose of the subsequent application to twisted wings, and with the root section as a reference,

$$(\alpha_{0r})_1 = 0.87(\alpha_{0r})_{\infty th} . \tag{3.9}$$

3.3 Evaluation of $(\alpha_{0r})_2$

Two cases will be considered; that for which the effective twist varies linearly with spanwise distance, in Section 3.3.1, and that for which the variation is non-linear, in Section 3.3.2.

3.3.1 Linear twist

For wings with linear spanwise twist distribution, Derivation 29 uses extended lifting-line theory to satisfy Equation (3.3) and give the change in the zero-lift angle of the wing root section due to twist at low speeds. Figures 1a to 1d present the results as carpets for $(\alpha_{0r})_2/\delta_{et}$ in terms of A and $A \tan\Lambda_{¼}$ for taper ratios $\lambda = 0$, 0.25, 0.5 and 1.0. For intermediate values of λ a cross-plot can be made but linear interpolation is felt to be adequate.

3.3.2 Non-linear twist

Equation (3.3) has been evaluated by simple strip theory for tapered wings with linear twist and non-linear twist in the form of "linear-lofted" twist (see Derivation 38), given by

$$\frac{\delta}{\delta_t} = \frac{\eta\lambda}{1-\eta(1-\lambda)}, \tag{3.10}$$

so as to maintain straight leading and trailing edges. The strip theory calculations suggest replacement of δ_{et} in Figures 1a to 1d by an equivalent linear twist

$$\delta'_{et} = \frac{3}{2}\delta_{e,\,2/3}, \tag{3.11}$$

where $\delta_{e,2/3}$ is the actual effective twist at $\eta = 2/3$. Good comparisons were obtained between calculations of $(\alpha_{0r})_2$ for wings with linear-lofted twist using vortex-lattice theory (in Derivation 38 using the method of Derivation 37) and similar calculations for the same wings using Figures 1a to 1d in conjunction with equivalent linear twist given by Equation (3.11).

The artifice in Equation (3.11) is likely to be adequate for twist distributions that are monotonic, as in the case of linear-lofted twist. For more complex twist distributions a method based on that given in Item No. 83040 (Derivation 39) should be used. The method of that Item represents the twist distribution by means of a series of linear segments. The following example gives the simple case in which the twist distribution can be represented by two linear segments.

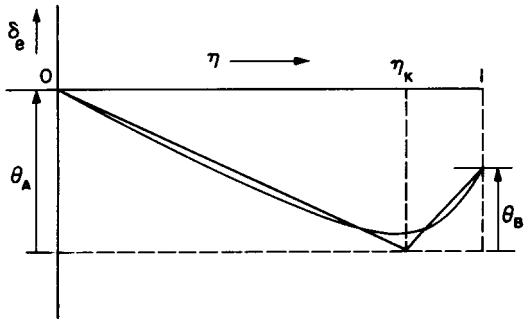

Sketch 3.1

The twist of type A, see Sketch 3.2, is defined as

$$\left.\begin{aligned} \theta &= \theta_A(\eta_K - \eta)/\eta_K && \text{for } 0 \le \eta \le \eta_K \\ &= 0 && \text{for } \eta_K \le \eta \le 1 \end{aligned}\right\} \tag{3.12}$$

and gives a lift coefficient C_{LTA} .

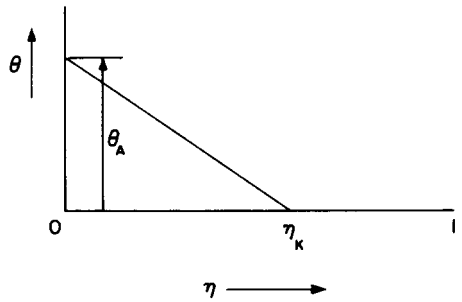

Sketch 3.2 Twist of type A

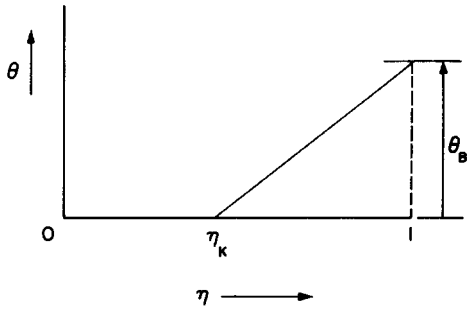

Sketch 3.3 Twist of type B

The twist of type B, see Sketch 3.3, is defined as

$$\left.\begin{aligned} \theta &= 0 && \text{for } 0 \le \eta \le \eta_K \\ &= \theta_B(\eta - \eta_K)/(1 - \eta_K) && \text{for } \eta_K \le \eta \le 1 \end{aligned}\right\} \tag{3.13}$$

and gives a lift coefficient C_{LTB} .

The representation by linear segments in Sketch 3.1 gives

$$\left.\begin{aligned} \delta_e &= -\theta_A + \theta_A(\eta_K - \eta)/\eta_K && \text{for } 0 \le \eta \le \eta_K \\ &= -\theta_A + \theta_B(\eta - \eta_K)/(1 - \eta_K) && \text{for } \eta_K \le \eta \le 1 \end{aligned}\right\} \tag{3.14}$$

and a corresponding lift coefficient

$$C_L = -\theta_A a_1 + \theta_A C_{LTA} + \theta_B C_{LTB}. \tag{3.15}$$

The contribution of the twist distribution to the zero-lift angle is

$$(\alpha_{0r})_2 = \theta_A - \theta_A \frac{C_{LTA}}{a_1} - \theta_B \frac{C_{LTB}}{a_1}. \tag{3.16}$$

The low-speed wing lift-curve slope, a_1 , can be obtained from Item No. 70011 (Reference 40). Alternatively, for the present purpose, sufficiently accurate values can be calculated from the simple equation

$$a_1 = \pi^2 A/\{90[2 + \sqrt{4 + (A\cos\Lambda_{¼})^2}]\}\,\text{deg}^{-1}, \tag{3.17}$$

obtained from Derivation 24, which provides values accurate to within about ±5 per cent of those given by Item No. 70011. The evaluation of $(\alpha_{0r})_2$ in Equation (3.16) also requires the values of C_{LTA} and C_{LTB}, which have been extracted from Item No. 83040, and are given in Tables 3.1 and 3.2, respectively, as functions of A and η_K.

Many practical twist distributions can be satisfactorily represented by only two linear segments. However, if more segments are required the method can be generalised to N segments as shown in Sketch 3.4

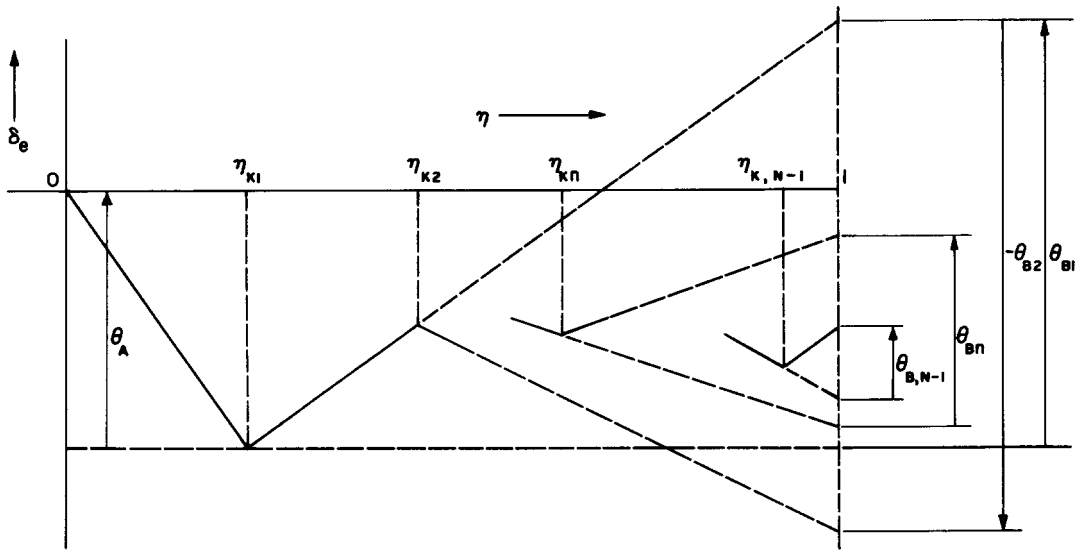

Sketch 3.4

From Sketch 3.4:-

$$\left.\begin{aligned} \delta_e &= -\theta_A + \theta_A(\eta_{K1} - \eta)/\eta_{K1} && \text{for } 0 \le \eta \le \eta_{K1} \\ &= -\theta_A + \sum_{i=1}^{n} \theta_{Bi}(\eta - \eta_{Ki})/(1 - \eta_{Ki}) && \text{for } \eta_{Kn} \le \eta \le \eta_{K,\,n+1} \end{aligned}\right\} \quad (3.18)$$

where $n = 1$ to $N - 1$ and $\eta_{KN} = 1$.

This representation gives

$$(\alpha_{0r})_2 = \theta_A - \theta_A \frac{C_{LTA}(\eta_{K1})}{a_1} - \sum_{n=1}^{N-1} \theta_{Bn} \frac{C_{LTB}(\eta_{Kn})}{a_1}, \quad (3.19)$$

which is a simple generalisation of Equation (3.16).

TABLE 3.1 Values of C_{LTA} (Derivation 39)

η_K \ A	1.5	3	5	8	12
0	0	0	0	0	0
0.1	0.0023	0.0036	0.0046	0.0054	0.0061
0.2	0.0045	0.0071	0.0091	0.0107	0.0119
0.3	0.0068	0.0106	0.0134	0.0158	0.0174
0.4	0.0089	0.0140	0.0176	0.0207	0.0226
0.5	0.0111	0.0173	0.0217	0.0254	0.0276
0.6	0.0131	0.0204	0.0256	0.0298	0.0323
0.7	0.0151	0.0234	0.0293	0.0339	0.0368
0.8	0.0170	0.0263	0.0327	0.0379	0.0409
0.9	0.0188	0.0289	0.0359	0.0415	0.0448
1.0	0.0203	0.0313	0.0388	0.0448	0.0483

TABLE 3.2 Values of C_{LTB} (Derivation 39)

η_K \ A	1.5	3	5	8	12
0	0.0150	0.0225	0.0270	0.0304	0.0330
0.1	0.0128	0.0192	0.0232	0.0263	0.0283
0.2	0.0108	0.0162	0.0195	0.0221	0.0238
0.3	0.0090	0.0134	0.0161	0.0182	0.0197
0.4	0.0072	0.0107	0.0129	0.0146	0.0158
0.5	0.0055	0.0082	0.0099	0.0112	0.0122
0.6	0.0040	0.0059	0.0071	0.0081	0.0089
0.7	0.0026	0.0039	0.0047	0.0054	0.0059
0.8	0.0014	0.0021	0.0026	0.0030	0.0033
0.9	0.0005	0.0008	0.0011	0.0013	0.0014
1.0	0	0	0	0	0

4. APPLICABILITY AND ACCURACY

The method given in this Item for estimating wing angle of attack for zero lift at subcritical Mach numbers is applicable to straight tapered wings with camber and twist provided that the local effective twist is not excessive ($\delta_e \leq 10°$, say) and provided that the flow over the wing is attached and wholly subsonic at the zero-lift condition. The method has been applied successfully to wings with cranked or curved edges by means of the "equivalent wing planform" concept detailed in Item No. 76003 (Reference 41).

The method can cope (via Item No. 72024) with any shape of camber line which may vary across the span. The method is capable of dealing with any form of spanwise twist distribution but is simplest to use for wings with an approximately linear twist distribution or for a twist distribution that is essentially monotonic. The method for the more complex twist distributions requires the values of C_{LTA} and C_{LTB} given in Tables 3.1 and 3.2, which are assumed to be invariant with $\Lambda_{¼}$ and λ. The tabulated values were in fact calculated for wings with $\Lambda_{¼} = 25°$ and $\lambda = 0.4$, but checks against values deduced using Figures 1a and

1b and Equation (3.16) for the special case of a single linear segment indicate that the assumption of invariance is reasonable (to within about ±10 per cent) for combinations of $\Lambda_{1/4}$ and λ within the hatched area shown in Sketch 4.1.

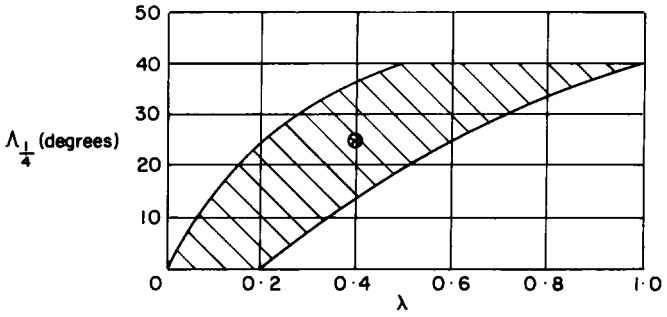

Sketch 4.1

It is recommended that, although for untwisted wings the method has been found to be independent of planform over very wide ranges of planform parameters, its use for twisted wings should be restricted to planforms in the range $\lambda \leq 1$, $2 \leq A \leq 10$ and $0 \leq A \tan \Lambda_{1/4} \leq 6$. For untwisted wings the upper limit on aspect ratio can be exceeded and moreover the method can be applied to wings with forward sweep.

The method has been compared with wind-tunnel test data for a wide range of aerofoils (Derivations 1 and 3 to 11) and wings, both without geometric twist (Derivations 12 to 23, 25 and 26) and with twist (Derivations 14 to 17, 23, 27, 28 and 30 to 36). The comparisons for low-speed flow are shown in Sketches 4.2, 4.3 and 4.4 for aerofoils, unswept wings and swept wings respectively. It is seen that while the test data for conventional NACA aerofoils correlate to within ±20 per cent, those for modern aerofoils correlate rather better, to within ±15 per cent. The data for wings are mainly correlated to within $\pm 0.3°$, independent of planform within the ranges noted earlier. The difference in the type of scatter exhibited by the test data for aerofoils (percentage) compared with that for wings (incremental) requires comment. To some extent the difference is a reflection of the fact that test data for wings relate to a smaller range of aerofoil sections than those covered by the two-dimensional tests. In this respect most of the wings represented in Sketches 4.3 and 4.4 had NACA 4- or 5-digit or NACA 6 or 6A sections, and with only two exceptions the corresponding two-dimensional test data were correlated to within $\pm 0.3°$. However, there were in addition 23 wings with sections (mostly pre-1940) that had not been represented in true two-dimensional tests and the data for these wings still correlated to within about $\pm 0.3°$ as shown. In spite of this evidence there is no reason to believe that test data for aerofoils are intrinsically less accurate than those for wings and in applying the method of this Item to wings it would be prudent to bear in mind the scatter relating to aerofoils (Sketch 4.2).

The effects of fixing boundary layer transition and of varying Reynolds number (provided that it is greater than about 10^6 based on $\bar{c}$) can be ignored within the quoted error bands.

It has been established by reference to theoretical calculations (Derivation 2) and test data (Derivations 1, 17, 18, 22, 35 and 36) that the angle of attack for zero lift of aerofoils and wings is essentially independent of Mach number up to the critical value. Where there is an effect it is often present as a slowly increasing reduction in the magnitude of α_{0r} as Mach number increases. Therefore, the method of this Item, although derived for low-speed flows, is applicable to subcritical Mach numbers. Confirmation of this is shown in Sketch 4.5 for a Mach number of 0.7.

Most of the data were restricted to straight tapered swept-back wings; exceptionally, Derivations 16 and 18 related to swept-forward wings without twist and Derivation 26 related to a wing with cranked trailing edges.

Conventional NACA aerofoils

Symbol	Family	NACA mean line
x	NACA 4-digit	64
+	NACA 5-digit	230
○	NACA 63	a = 1
□	NACA 64	a = 1
△	NACA 65	a = 1
▽	NACA 66	a = 1
●	NACA 63	a = 0·3
▲	NACA 65	a = 0·5, 0·6, 0·8
▼	NACA 66	a = 0·6
◐	NACA 63A	a = 0·8 (mod)
◧	NACA 64A	a = 0·8 (mod)
◇	Modern aerofoils	

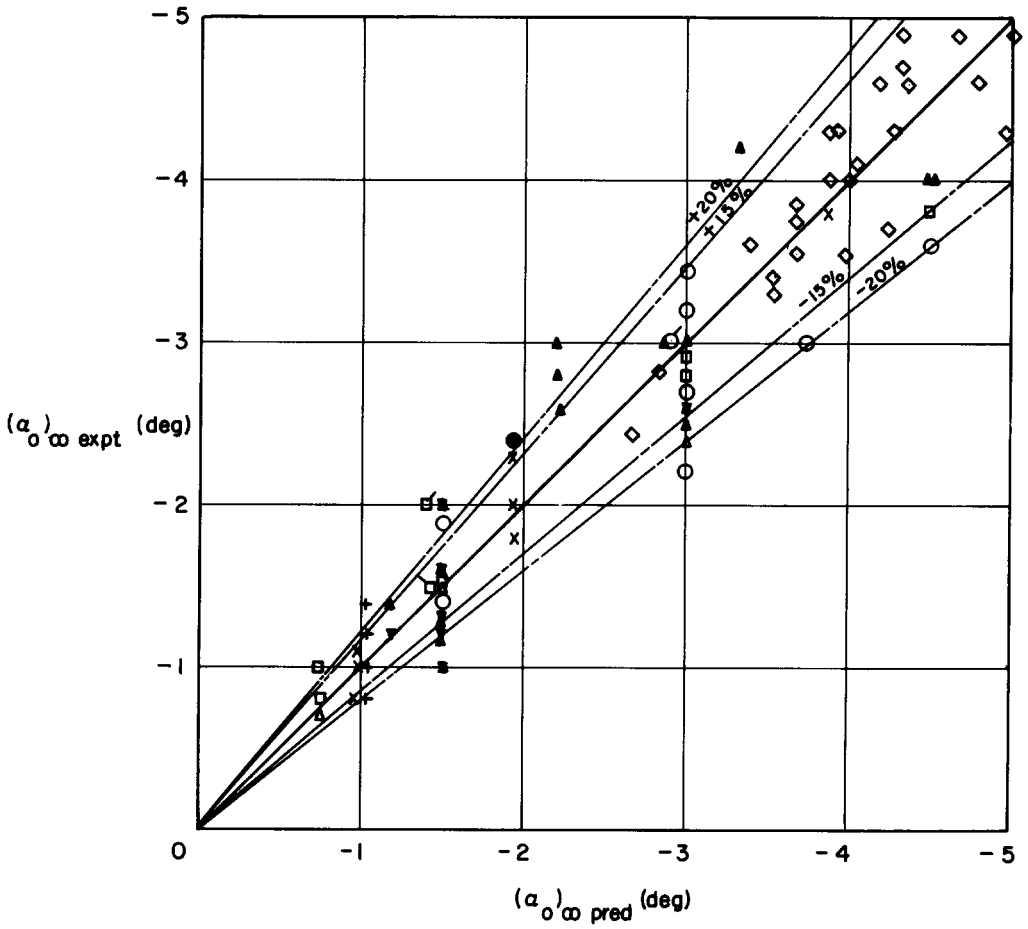

Sketch 4.2 Correlation of method with test data for aerofoils at low speeds

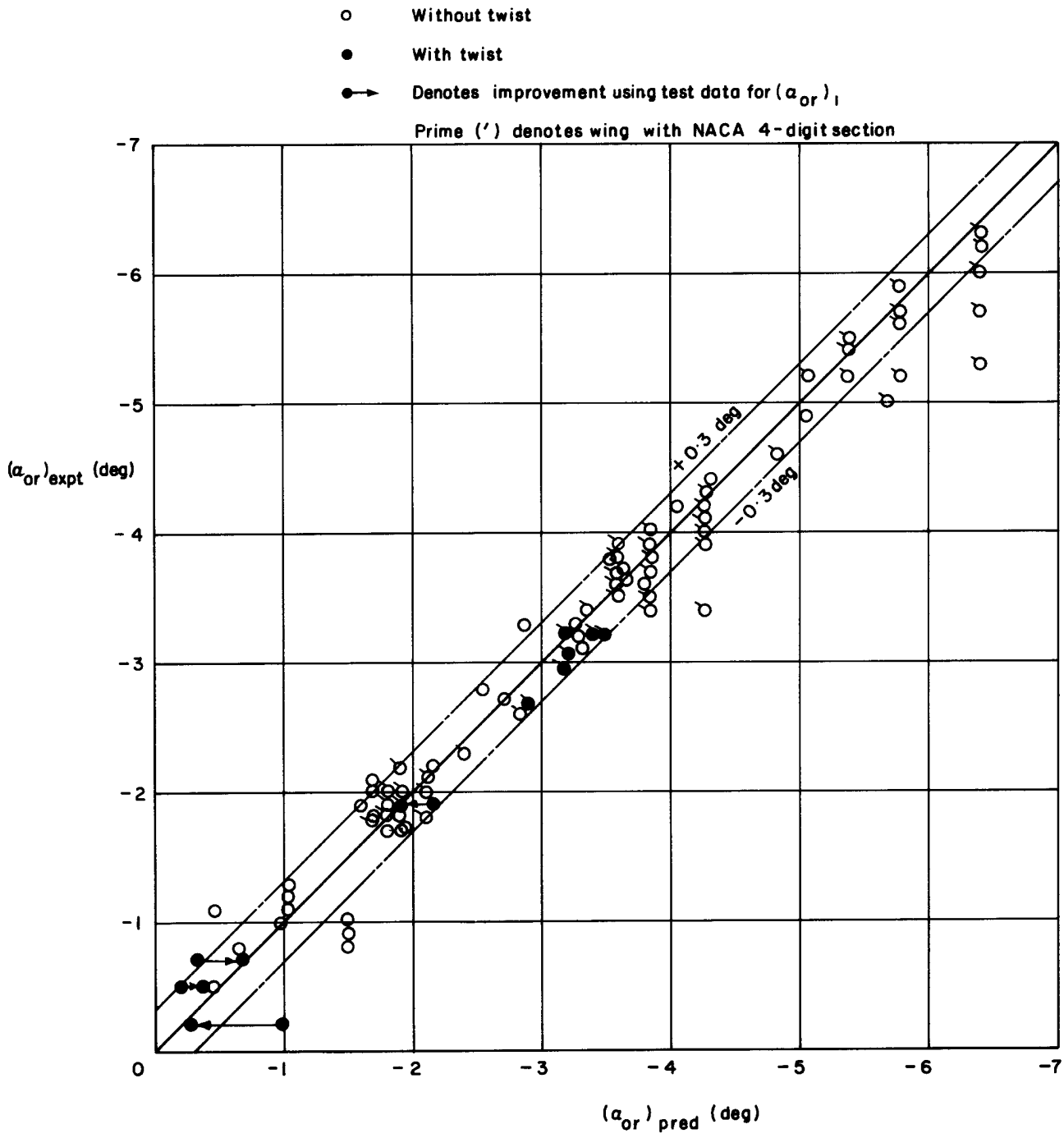

Sketch 4.3 Correlation of method with test data for unswept wings ($\Lambda_{1/4} = 0$) at low speeds

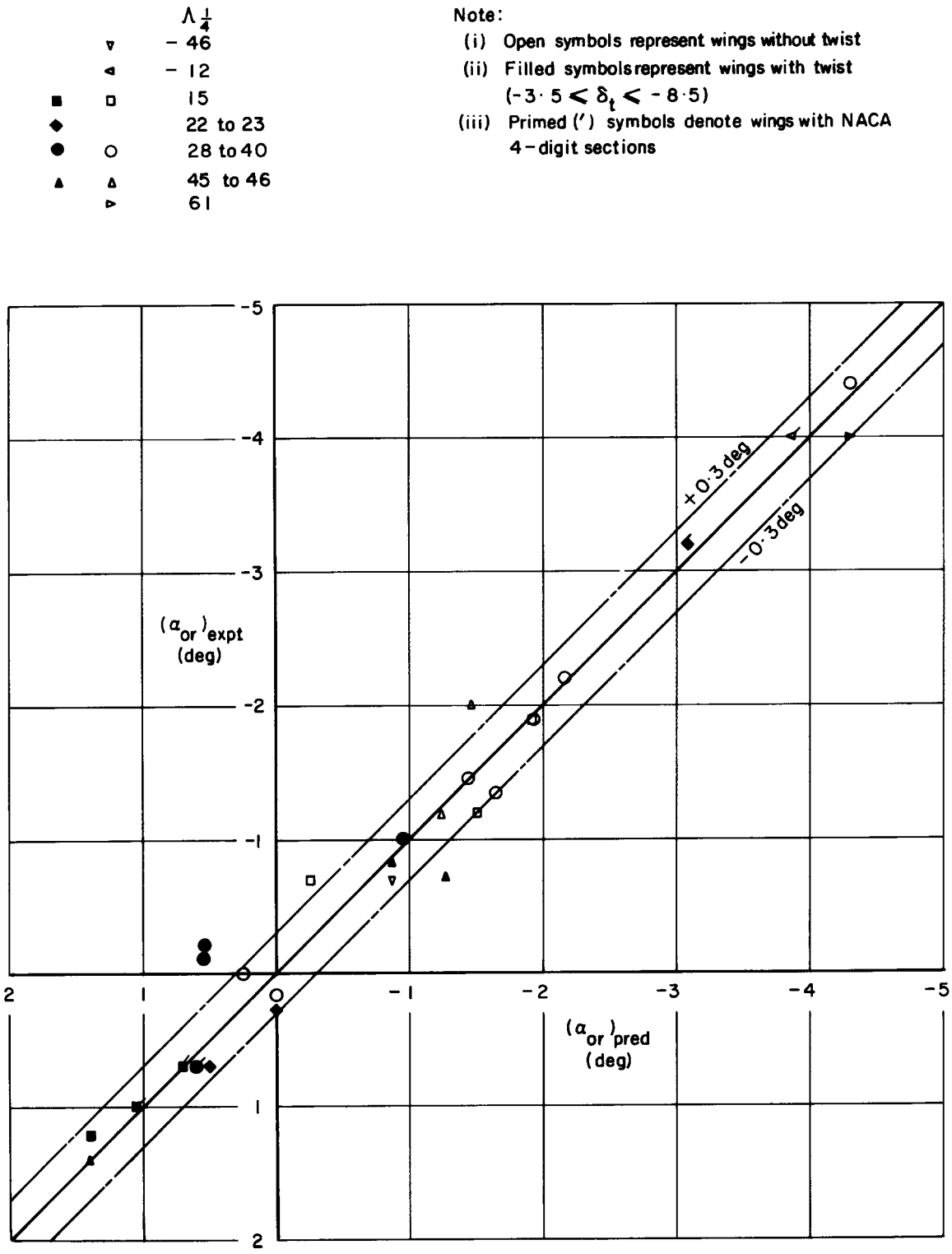

Sketch 4.4 Correlation of method with test data for swept wings ($\Lambda_{\frac{1}{4}} \neq 0$) at low speeds

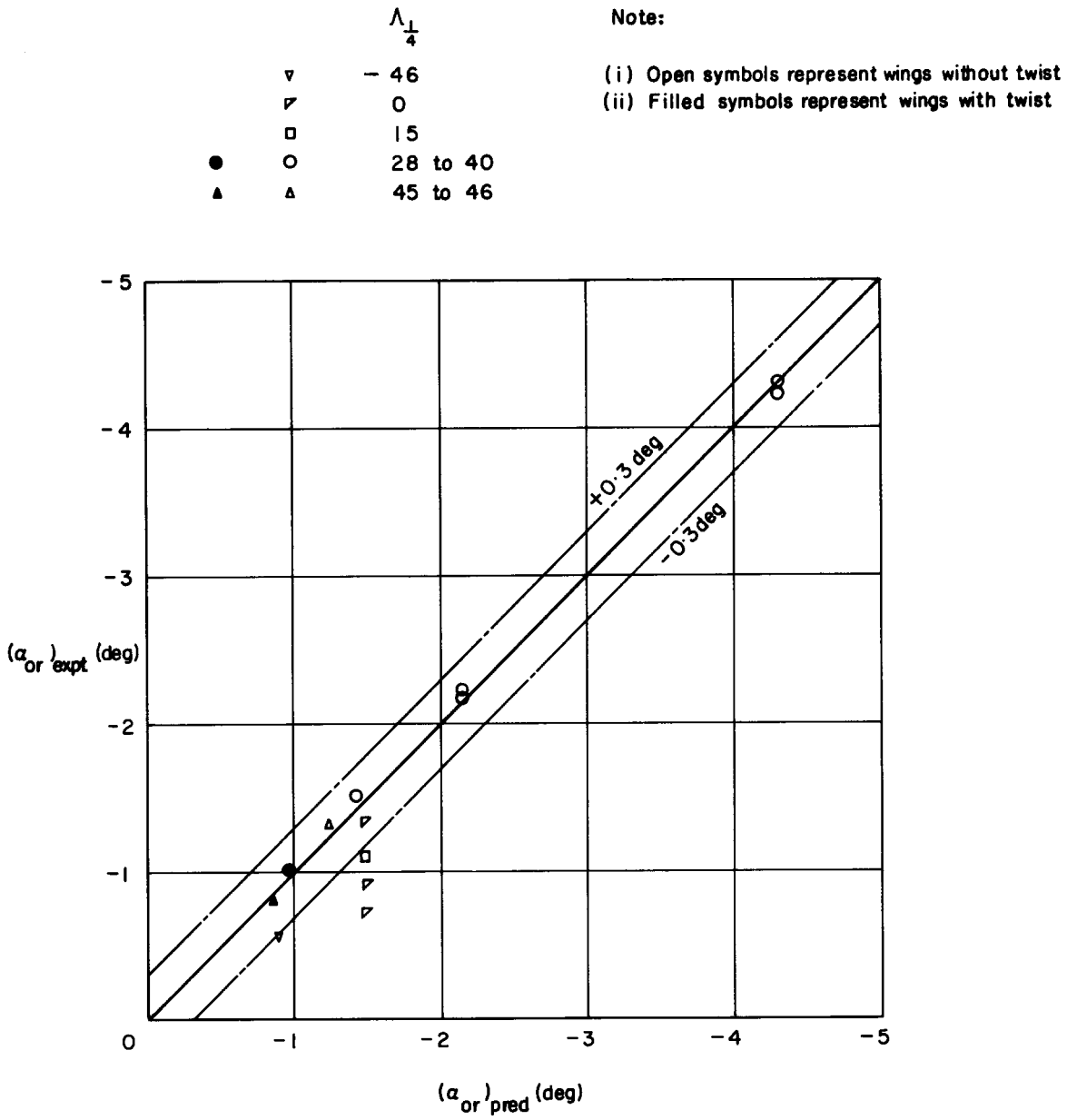

Sketch 4.5 Correlation of method with test data for wings at Mach number of 0.7

5. DERIVATION AND REFERENCES

5.1 Derivation

The Derivation lists selected sources that have assisted in the preparation of this Item.

Aerofoils

1. ABBOTT, I.H. VON DOENHOFF, A.E. — THEORY OF WING SECTIONS. Published by Dover Publications Inc., New York, 1959.
2. ESDU — Aerodynamic characteristics of aerofoils in compressible inviscid airflow at subcritical Mach numbers. Item No. 72024. ESDU International, 1972.
3. McGHEE, R.J. BEASLEY, W.D. — Low speed aerodynamic characteristics of a 17-percent-thick airfoil section designed for general aviation applications. NASA tech. Note D-7428, 1973.
4. McGHEE, R.J. BEASLEY, W.D. — Effect of thickness on the aerodynamic characteristics of an initial low-speed family of airfoils for general aviation applications. NASA tech. Memor. 72843, 1976.
5. McGEE, R.J. BEASLEY, W.D. — Low speed wind tunnel results for a modified 13-percent-thick airfoil. NASA tech. Memor.-X 74018, 1979.
6. McGEE, R.J. BEASLEY, W.D. — Wind tunnel results for an improved 21-percent-thick low-speed airfoil section. NASA tech. Memor. 78650, 1978.
7. ALTHAUS, D. WORTMANN, F.X. — STUTTGARTER PROFILKATALOG I. Published by F.Vieweg and Son, Braunschweig/Wiesbaden, 1979.
8. McGHEE, R.J. BEASLEY, W.D. — Low speed aerodynamic characteristics of a 13-percent-thick medium speed airfoil designed for general aviation applications. NASA tech. Paper 1498, 1979.
9. HARRIS, C.D. BEASLEY, W.D. — Low speed aerodynamic characteristics of a 14-percent-thick NASA phase 2 supercritical airfoil designed for a lift coefficient of 0.7. NASA tech. Memor. 81912, 1980.
10. McGHEE, R.J. BEASLEY, W.D. — Low speed aerodynamic characteristics of a 17-percent-thick medium speed airfoil designed for general aviation applications. NASA tech. Paper 1786, 1980.
11. McGHEE, R.J. BEASLEY, W.D. — Wind tunnel results for a modified 17-percent-thick low-speed airfoil section. NASA tech. Paper 1919, 1981.

Wings with Camber

12. ANDERSON, R.F. — The aerodynamic characteristics of airfoils at negative angles of attack. NACA tech. Note 412, 1932.
13. JACOBS, E.N. WARD, K.E. PINKERTON, R.M. — The characteristics of 78 related airfoil sections from tests in the variable density wind tunnel. NACA Rep. 460, 1933.

14. ANDERSON, R.F. — Determination of the characteristics of tapered wings. NACA Rep. 572, 1936.

15. ANDERSON, R.F. — The experimental and calculated characteristics of 22 tapered wings. NACA Rep. 627, 1938.

16. MENDELSOHN, R.A. BREWER, J.D. — Comparison between the measured and theoretical span loading on a moderately swept-forward and a moderately swept-back semispan wing. NACA tech. Note 1351, 1946.

17. HAMILTON, W.T. NELSON, W.H. — Summary report on the high speed characteristics of six model wings having NACA 65-series sections. NACA Rep. 877, 1947.

18. HIESER, G. WHITCOMB, C.F. — Investigation of the effects of a nacelle on the aerodynamic characteristics of a swept wing and the effects of sweep on a wing alone. NACA tech. Note 1709, 1948.

19. HOPKINS, E.J. — A wind-tunnel investigation at low speed of various lateral controls on a 45° swept-back wing. NACA RM A7L16 (TIL 1613), 1948.

20. ANSCOMBE, A. RANEY, D.J. — Low speed tunnel investigation of the effect of the body on C_{mo} and aerodynamic centre of unswept wing-body combinations. ARC CP 16, 1950.

21. RILEY, D.R. — Wind tunnel investigation and analysis of the effects of end plates on the aerodynamic characteristics of an unswept wing. NACA tech. Note 2440, 1951.

22. TINLING, B.E. KOLK, W.R. — The effects of Mach number and Reynolds number on the characteristics of several 12-percent-thick wings having 35° of sweepback and various amounts of camber. NACA RM A50K27 (TIL 2629), 1951.

23. ROSE, L.M. — Low-speed characteristics of a wing having 63° sweepback and uniform camber. NACA RM A51D25 (TIL 2781), 1951.

24. LOWRY, J.G. POLHAMUS, E. — A method for predicting lift increments due to flap deflections at low angles of attack in incompressible flow. NACA tech. Note 3911, 1957.

25. BREBNER, G.G. WYATT, L.A. ILOTT, G.P. — Low speed wind tunnel tests on a series of rectangular wings of varying aspect ratio and aerofoil section. ARC CP 916, 1967.

26. LOVELL, D.A. — A wind-tunnel investigation of the effects of flap span and deflection angle, wing planform and a body on the high-lift performance of a 28° swept wing. RAE tech. Rep. 76030, 1976.

Wings with Camber and Geometric Twist

27. CONNER, D.W. — Effect of reflex camber on the aerodynamic characteristics of a highly tapered moderately swept-back wing at Reynolds numbers up to 8,000,000. NACA tech. Note 1212, 1946.

28. NEELY, R.H. BOLLECH, T.V. WESTRICK, G.C. GRAHAM, R.R. — Experimental and calculated characteristics of several NACA 44-series wings with aspect ratios of 8, 10 and 12 and taper ratios of 2.5 and 3.5. NACA tech. Note 1270, 1974.

29. DeYOUNG, J. HARPER, C.W. — Theoretical symmetric span loading at subsonic speeds for wings having arbitrary planform. NACA Rep. 921, 1948.

30. BOLLECH, T.V. — Experimental and calculated characteristics of several high-aspect-ratio tapered wings incorporating NACA 44-series, 230-series and low-drag 64-series airfoil sections. NACA tech. Note 1677, 1948.

31. SIVELLS, J.C. SPOONER, S.H. — Investigation in the Langley 19-foot pressure tunnel of two wings of NACA 65-210 and 64-210 airfoil sections with various type flaps. NACA Rep. 942, 1949.

32. TROUNCER, J. KETTLE, D. — Low speed model tests on two “V” wings. ARC R & M 2364, 1950.

33. JAQUET, B.M. — Effect of linear spanwise variations of twist and circular-arc camber on low-speed static stability, rolling, and yawing characteristics of a 45° sweptback wing of aspect ratio 4 and taper ratio 0.6. NACA tech. Note 2775, 1952.

34. SALMI, R.J. — Low-speed longitudinal aerodynamic characteristics of a twisted and cambered wing of 45° sweepback and aspect ratio 8 with and without high-lift and stall-control devices and a fuselage at Reynolds numbers from 1.5×10^6 to 4.8×10^6. NACA RM L52C11 (TIL 3192), 1952.

35. BOLTZ, F.W. KOLBE, C.D. — The forces and pressure distribution at subsonic speeds on a cambered and twisted wing having 45° of sweepback, an aspect ratio of 3 and a taper ratio of 0.5. NACA RM A52D22 (TIL 3268), 1952.

36. EDWARDS, G.G. TINLING, B.E. ACKERMAN, A.C. — The longitudinal characteristics at Mach numbers up to 0.92 of a cambered and twisted wing having 40° of sweepback and an aspect ratio of 10. NACA RM A52F18 (TIL 3318), 1952.

37. MARTIN, G.W. — Vortex collocation lifting surface theory for subsonic compressible potential flow. Lockheed-Georgia Co, Engineering Report ER-8814, 1967.

38. GILMAN, B.G. BURDGES, K.P. — Rapid estimation of wing aerodynamic characteristics for minimum induced drag. J. Aircr., Vol. 4, No. 6, November - December 1967, pp. 563-565.

39. ESDU — Method for the rapid estimation of spanwise loading of wings with camber and twist in subsonic attached flow. Item No. 83040. ESDU International, 1983.

5.2 References

The References list sources of information supplementary to that given in this Item.

40. ESDU — Lift-curve slope and aerodynamic centre position of wings in inviscid subsonic flow. Item No. 70011. ESDU International, 1970.

41. ESDU — Geometrical properties of cranked and straight tapered wing planforms. Item No. 76003. ESDU International, 1976.

42. ESDU Wing pitching moment at zero lift at subcritical Mach numbers. Item No. 87001. ESDU International, 1987.

43. ESDU Aerofoil incidence for zero lift in subsonic two-dimensional flow. Item No. 98011. ESDU International, 1997.

6. EXAMPLES

6.1 Example 1

The angle of attack at zero lift for subcritical Mach numbers is required for the wing shown in Sketch 6.1. The planform parameters for the equivalent wing, shown dotted, are $A = 7$, $\Lambda_{1/4} = 25°$ and $\lambda = 0.3$. The wing has a fixed section with the shape of camber line in Sketch 6.1 and ordinates in Table 6.1. The wing has a linear-lofted spanwise distribution of twist, given by Equation (3.10) and shown in Sketch 6.1, with a tip value $\delta_t = -3°$.

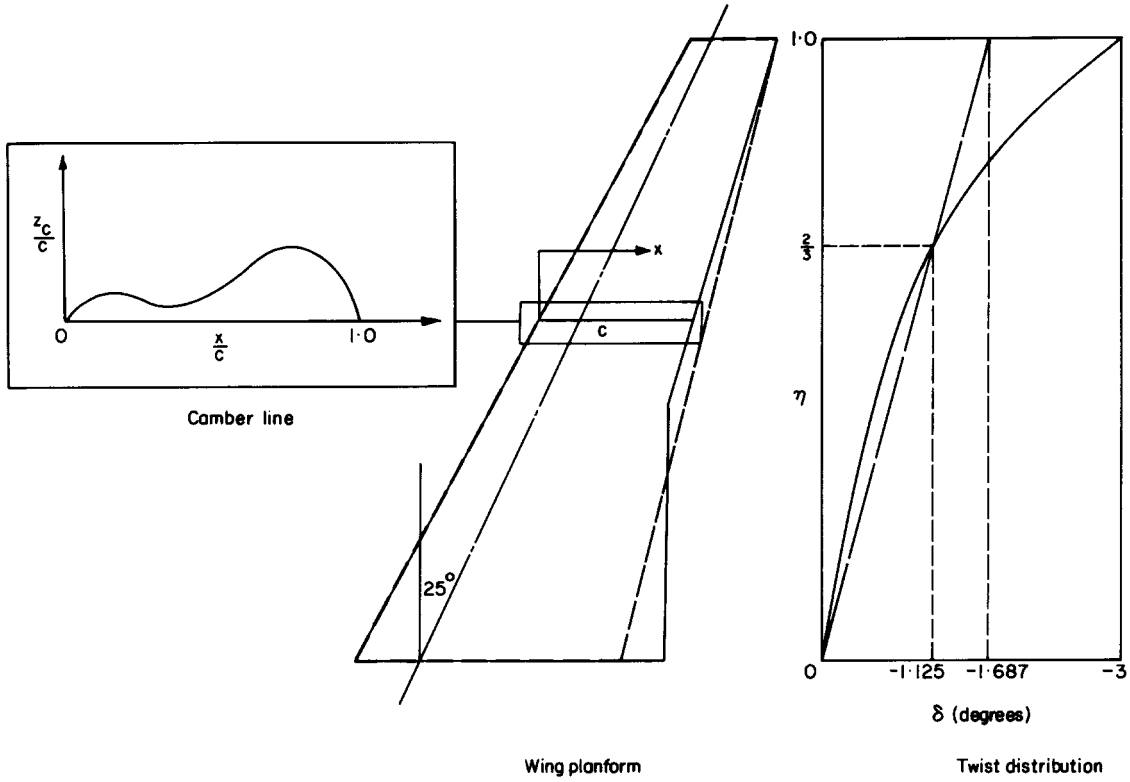

Sketch 6.1

TABLE 6.1 Camber line ordinates

x/c	z_c/c
0.0	0.0
0.025	0.0028
0.050	0.0037
0.1	0.0045
0.2	0.0038
0.3	0.0022
0.4	0.0020

x/c	z_c/c
0.5	0.0047
0.6	0.0082
0.7	0.0104
0.8	0.0105
0.9	0.0079
0.95	0.0050
1.0	0.0

Use of Addendum A of Item No. 72024 (Derivation 2) gives, for the camber line ordinates in Table 6.1,

$$(\alpha_0)_{\infty th} = (\alpha_{0r})_{\infty th} = -1.93 \text{ degrees.}$$

Therefore, from Equation (3.9),

$$(\alpha_{0r})_1 = 0.87(\alpha_{0r})_{\infty th} = 0.87 \times (-1.93) = -1.68 \text{ degrees.}$$

For linear-lofted twist, Equation (3.10) for $\lambda = 0.3$ and $\delta_t = -3°$ becomes

$$\delta = -0.9\eta/(1-0.7\eta) \text{ degrees,}$$

which, for $\eta = 2/3$, gives

$$\delta_{2/3} = \delta_{e,\,2/3} = -1.125 \text{ degrees.}$$

Equation (3.11) therefore gives,

$$\delta'_t = \delta'_{et} = \frac{3}{2}\delta_{e,\,2/3} = \frac{3}{2} \times (-1.125) = -1.687 \text{ degrees.}$$

From Figures 1a and 1b, with $A = 7$ and $A\tan\Lambda_{¼} = 7 \times \tan 25° = 3.26$, interpolation for $\lambda = 0.3$ in a cross-plot gives,

$$\frac{(\alpha_{0r})_2}{\delta_{et}} = -0.387,$$

which, with δ_{et} replaced by $\delta'_{et} = -1.687$ degrees, gives

$$(\alpha_{0r})_2 = -0.387 \times (-1.687) = 0.65 \text{ degrees.}$$

Hence, from Equation (3.2)

$$\alpha_{0r} = (\alpha_{0r})_1 + (\alpha_{0r})_2 = -1.68 + 0.65 = -1.03 \text{ degrees.}$$

It can be seen that the effect of twist is to offset the camber contribution to angle of attack at zero lift by nearly 40 per cent.

6.2 Example 2

In order to alleviate the nose-down pitching moment at zero lift for the wing of Example 1 (see Example 1 of Item No. 87001) the camber line at the wing tip is maintained but the camber ordinates in Table 6.1 are reduced linearly to zero at the wing root. Find the effect of this on the angle of attack at zero lift.

Because the camber ordinates are proportional to η

$$(\alpha_{0\eta})_{\infty} = \eta(\alpha_{0t})_{\infty},$$

where $(\alpha_{0t})_{\infty} = -1.68$ degrees (from Example 1). So, for $\eta = 0$ and 2/3

$$(\alpha_{0r})_{\infty} = (\alpha_{0r})_1 = 0$$

and $$(\alpha_{0,2/3})_{\infty} = \frac{2}{3}\times(-1.68) = -1.12 \text{ degrees.}$$

Thus, from Equation (3.5), with these values and $\delta_{2/3} = -1.125$ degrees (from Example 1),

$$\begin{aligned}\delta_{e,2/3} &= \delta_{2/3} + (\alpha_{0r})_{\infty} - (\alpha_{0,2/3})_{\infty} \\ &= -1.125 + 0 - (-1.12) \\ &= -0.005 \text{ degrees.}\end{aligned}$$

Equation (3.11) now gives

$$\delta'_{et} = \frac{3}{2}\delta_{e,2/3} = \frac{3}{2}\times(-0.005) = -0.0075 \text{ degrees.}$$

From Example 1,

$$(\alpha_{0r})_2/\delta'_{et} = -0.387$$

giving $$(\alpha_{0r})_2 = -0.387\times(-0.0075) = 0.003 \text{ degrees.}$$

Hence, from Equation (3.2),

$$\alpha_{0r} = (\alpha_{0r})_1 + (\alpha_{0r})_2 = 0 + 0.003 \approx 0\,.$$

It can be seen that the spanwise variation of camber adopted has changed the angle of attack at zero lift from –1.03 degrees to nearly zero.

6.3 Example 3

The angle of attack at zero lift is required for the wing with $A = 4$, $\Lambda_{¼} = 30°$ and $\lambda = 0.4$, having the camber line of the wing in Example 1 and the spanwise variation of geometric twist shown in Sketch 6.2.

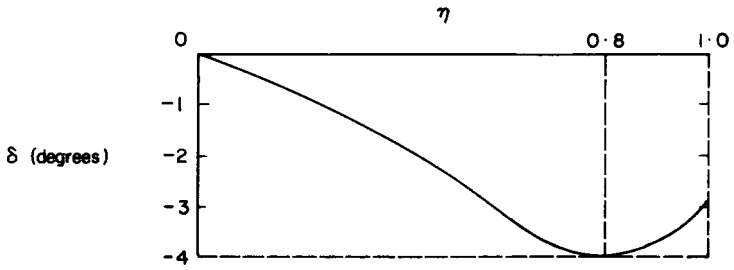

Sketch 6.2

From Example 1

$$(\alpha_{0r})_1 = -1.68 \text{ degrees.}$$

The twist distribution in Sketch 6.2 can be approximately represented by two linear segments with $\eta_K = 0.8$, $\theta_A = 4$ degrees and $\theta_B = 1$ degree as shown in Sketch 6.3.

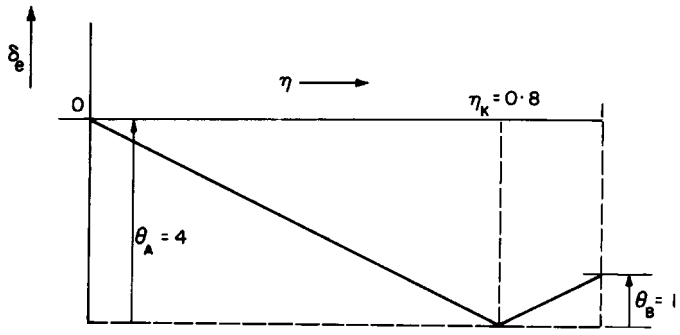

Sketch 6.3

From Equation (3.17),

$$a_1 = \pi^2 A \Big/ \left\{ 90 \left[2 + \sqrt{4 + (A/\cos\Lambda_{¼})^2} \right] \right\}$$

$$= \pi^2 \times 4 \Big/ \left\{ 90 [2 + \sqrt{4 + (4/\cos 30°)^2}] \right\}$$

$$= 0.0624 \text{ degree}^{-1}.$$

(This compares with a value of 0.0621 degree^{-1} from Item No. 70011.)

From Tables 3.1 and 3.2 for $\eta_K = 0.8$, interpolation for $A = 4$ in a cross-plot gives

$$C_{LTA} = 0.0300 \text{ and } C_{LTB} = 0.0024.$$

Therefore, from Equation (3.16)

$$(\alpha_{0r})_2 = \theta_A - \theta_A \frac{C_{LTA}}{a_1} - \theta_B \frac{C_{LTB}}{a_1}$$

$$= 4 - 4 \times \frac{0.0300}{0.0624} - 1 \times \frac{0.0024}{0.0624}$$

$$= 2.04 \text{ degrees.}$$

So that, from Equation (3.2)

$$\alpha_{0r} = (\alpha_{0r})_1 + (\alpha_{0r})_2$$

$$= -1.68 + 2.04$$

$$= 0.36 \text{ degrees.}$$

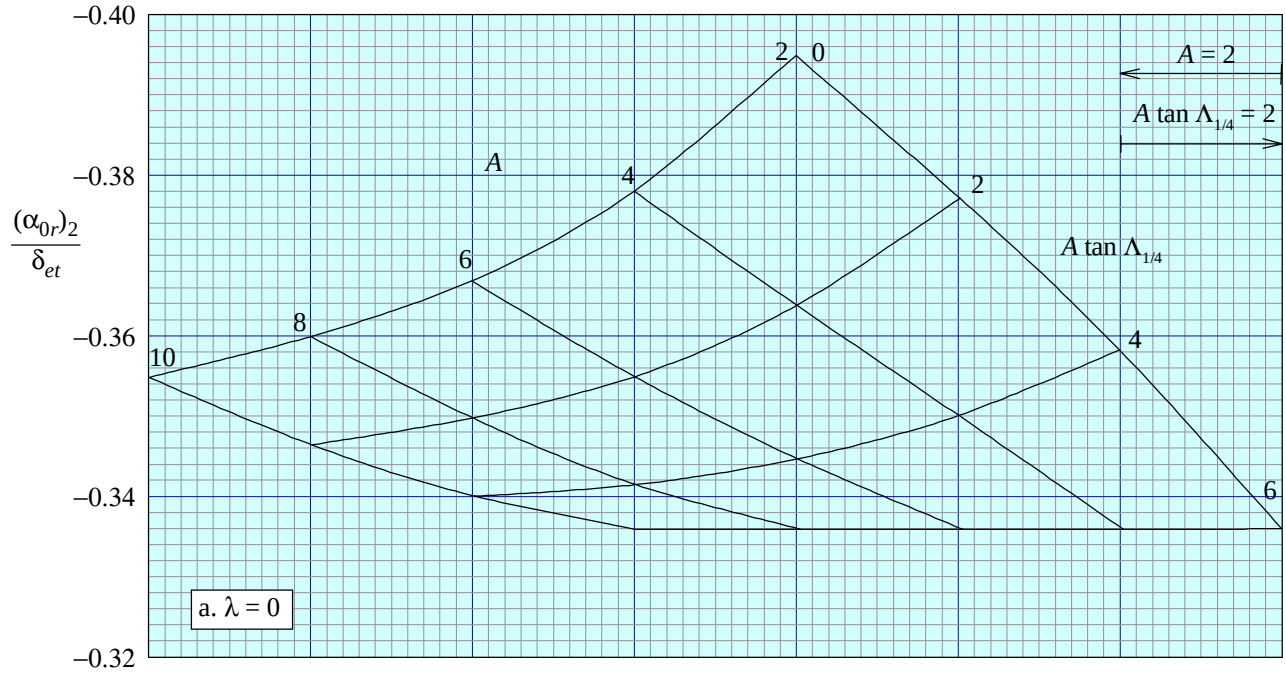

FIGURE 1a

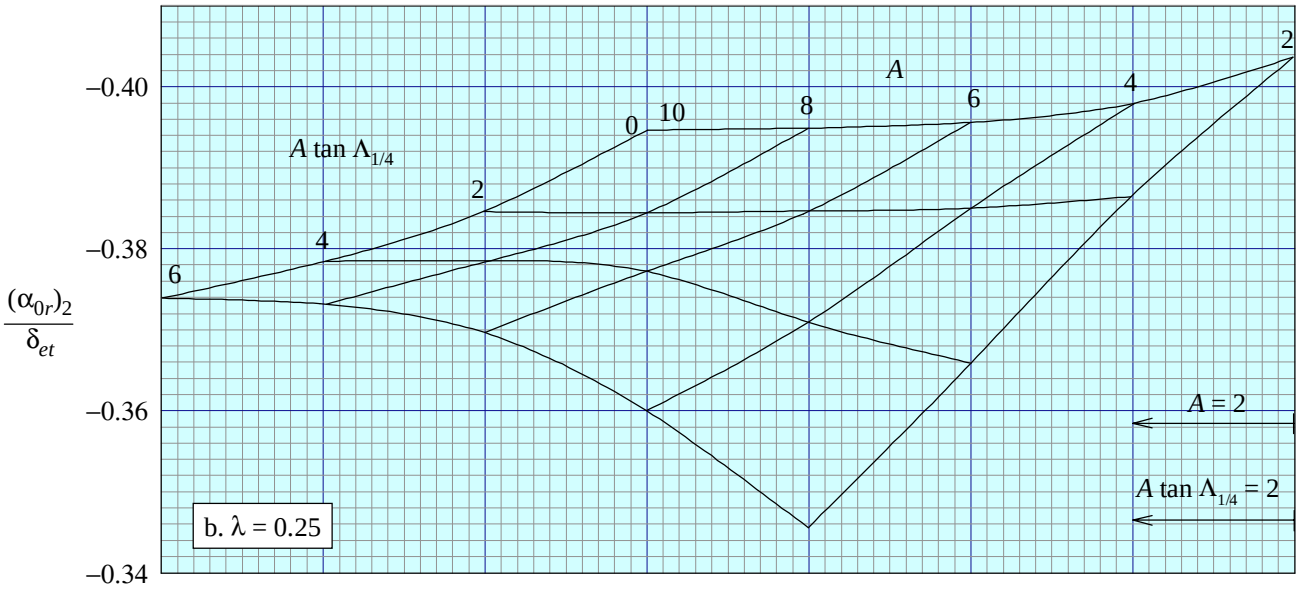

FIGURE 1b

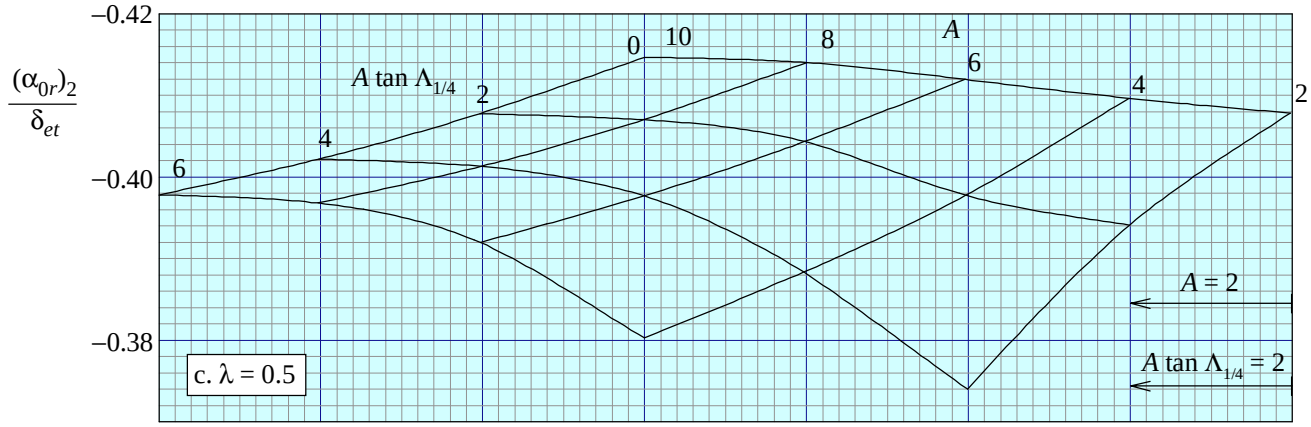

FIGURE 1c

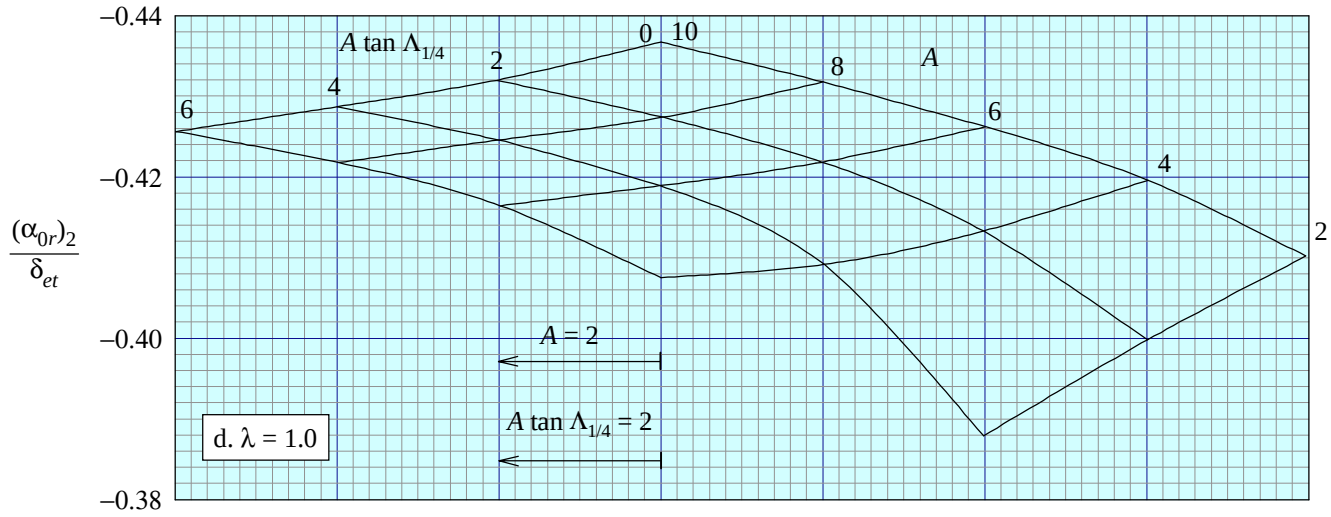

FIGURE 1d

This page Amendment A

THE PREPARATION OF THIS DATA ITEM

The work on this particular Item was monitored and guided by the Aerodynamics Committee which first met in 1942 and now has the following membership:

Chairman

Mr H.C. Garner	– Independent

Vice-Chairman

Mr P.K. Jones	– British Aerospace plc, Civil Aircraft Div., Woodford

Members

Mr G. Bean*	– Boeing Aerospace Company, Seattle, Wash., USA
Mr E.A. Boyd	– Cranfield Institute of Technology
Mr K. Burgin	– Southampton University
Dr T.J. Cummings	– Short Brothers plc
Mr J.R.J. Dovey	– Independent
Mr L. Elmeland*	– Saab-Scania, Linköping, Sweden
Dr J.W. Flower	– Bristol University
Mr P.G.C. Herring	– Sowerby Research Centre, Bristol
Mr R. Jordan	– Aircraft Research Association
Mr J.R.C. Pedersen	– Independent
Mr N. Roberts	– Rolls-Royce plc, Derby
Mr R. Sanderson	– Messerschmitt-Bölkow-Blohm GmbH, Hamburg, W. Germany
Mr A.E. Sewell*	– McDonnell Douglas, Long Beach, Calif., USA
Mr M.R. Smith	– British Aerospace plc, Military Aircraft Div., Weybridge
Miss J.Willaume	– Aérospatiale, Toulouse, France.

* Corresponding Member

The technical work involved in the assessment of the available information and the construction and subsequent development of the Data Item was undertaken by

Mr P. D. Chappell	– Head of Aircraft Aerodynamics, Group.